Available online at www.sciencedirect.com
SCIENCE DIRECT®
Journal of Sound and Vibration 274 (2004) 1013–1029
JOURNAL OF SOUND AND VIBRATION
www.elsevier.com/locate/jsvi

Non-linear vibration of initially stressed hybrid composite plates

Chun-Sheng Chen[a], Chin-Ping Fung[b,*]

[a] Department of Mechanical Engineering, Lunghwa Science and Technology University, Guai-Shan 33327, Taiwan
[b] Department of System Engineering, Chung Cheng Institute of Technology, Tao-Yuan 33509, Taiwan

Received 10 May 2002; accepted 9 June 2003

Abstract

Non-linear partial differential equations based on the Reissner–Mindlin plate theory are derived for large amplitude vibration of a hybrid composite plate in a general state of non-uniform initial stress. The equations include the effects of transverse shear and rotary inertia. Using these derived governing equations, the large amplitude vibration of an initially stressed hybrid composite plate is studied. The initial stress is taken to be a combination of pure bending stress and a uniform normal stress in the plane of the plate. The Galerkin method is used to reduce the governing non-linear partial differential equations to ordinary non-linear differential equations and the Runge–Kutta method is used to obtain the non-linear frequencies. The linear frequency can be obtained by neglecting the non-linear terms in ordinary non-linear differential equations. The non-linear vibration frequencies are sensitive to the vibration amplitude, elastic modulus, laminate stacking sequence and state of initial stresses. The effects of various parameters on the large amplitude free vibrations are presented.

1. Introduction

Composite materials have been used successfully in many engineering applications. However, the non-linear vibration of composite materials is still a major concern to engineers and it is necessary to understand the topic more. The non-linear vibration analysis of von Karman's equations for laminated plate was presented by Chandra [1] and Chandra and Raju [2]. They presented the non-linear free vibration behavior of an unsymmetrically stacked angle- and cross-ply laminated plates using Berger's assumption and perturbation method. Berger's assumption

*Corresponding author. Tel.: +886-3-380-9257; fax: +886-3390-6385.
E-mail address: cpfung@ccit.edu.tw (C.-P. Fung).

0022-460X/$ - see front matter © 2003 Elsevier Ltd. All rights reserved.
doi:10.1016/S0022-460X(03)00661-8

had been employed to study the large amplitude vibration of thick plates [3]. It was found that the transverse shear and rotary inertia play considerably important roles [4]. Reddy and Chao [5] and Reddy et al. [6] applied finite element method to the non-linear vibration theory that includes transverse shear strains, and studied the rectangular plates of angle- and cross-ply. The large amplitude free vibration of generally laminated anisotropic plates was studied by Sivakumaran and Chia [7]. A direct numerical integration method with harmonic oscillations assumption was applied to study the large amplitude vibration behaviour of cross-ply plate [8,9].

Rao and Pillai [10] and Rao [11] presented an equation of motion for the non-linear effects that have long been recognized as an important role in the vibration analysis of many thin structures. Argyris et al. [12] used the natural mode method for finite element analysis of composite structure. The large amplitude vibration of composite plates is investigated. Sinfh [13] presented the non-linear vibration of laminated plates using the Ralyleigh–Ritz method. The influences of the large amplitude and the geometry on the natural frequency are examined. Mackerle presents a bibliography of references on finite element method applied to the analysis of non-linear problems [14,15]. All these previous studies considered only plates of one material. Few studies have yet been undertaken on the non-linear vibration of hybrid composite. However, hybrid composite is a quite important material. Pure metal material can be replaced by it to save weight. Hybrid composite such as fiber reinforced polymer covered by metal can also enhance wear resistance and it was applied to rocket launcher successfully. The non-linear vibration of laminated hybrid composite plates was studied by Lee and Kim [16]. In his work, the effects of laminate stacking sequences, aspect ratios and number of layers on the non-linear vibration were investigated.

Non-linear vibration of plates under various initial stresses often happens in engineering applications. Brunelle and Robertson [17,18] studied the effects of arbitrary initial stress vibration problems using the average stress method and the variation method. Based on various plate theories, the effects of an arbitrary state of initial stress on large amplitude vibration problems of isotropic plate were studied [19–22]. Grawford and Atluri [23] analyzed the non-linear vibration of plates with initial stress. Cheung et al. [24] used the finite strip method to analyze non-linear vibration of plates with initial stresses. Yamaki and Chiba [25] and Yamaki et al. [26] presented the analysis and experiment for non-linear vibration of a clamped plate with initial deflection. The large amplitude vibration analysis of hybrid composite plates in an arbitrary state of initial stress is sparse. In the present study, non-linear vibration of laminated hybrid composite plates in an arbitrary state of initial stress is investigated. The effects of transverse shear strain and rotary inertia were both included in governing equations. The governing equations are derived by the average stress method on the basis of Von Karman assumptions. The Galerkin's approximate method is applied to the governing partial differential equations to generate five ordinary differential equations. The ordinary differential equations are solved by the Runge–Kutta method. The effects of initial condition, stacked types and vibration amplitude on frequency ratio are studied.

2. Perturbed equations

A body, which is in static equilibrium and subjected to a time-varying incremental deformation is considered with a non-uniform initial stress. The methodology described by Bolotin [27] and

Chen et al. [21] was employed, in which the governing equations were derived in Cartesian rectangular co-ordinates using a perturbing technique. The governing equations in the same form as Eqs. (1) and (2) of Ref. [17] are as follows:

$$(\sigma_{ij}\bar{u}_{s,j})_{,i} + [\bar{\sigma}_{ij}(\delta_{ij} + u_{s,j} + \bar{u}_{s,j})]_{,i} + \bar{F}_s + \Delta F_s = \rho\ddot{\bar{u}}_s, \tag{1}$$

$$\bar{P}_s + \Delta P_s = [\sigma_{ij}\bar{u}_{s,j} + \bar{\sigma}_{ij}(\delta_{js} + u_{s,j} + \bar{u}_{s,j})]n_i, \tag{2}$$

where σ_{ij}, $\bar{\sigma}_{ij}$, $\bar{F}_s$ and $\bar{P}_s$ are the initial stress, perturbing stress, body force and applied surface traction, respectively. The u_s and $\bar{u}_s$ represent the initial displacement and the incremental displacement, respectively. The terms ΔP_s and ΔF_s represent the changes of the initial surface traction and body force due to the perturbation. The n_i are the components of the unit normal given with respect to the spatial frame. It is assumed that the initial displacement gradients are so small that the product $\bar{\sigma}_{ij}u_{s,j}$ can be neglected. For the plate theory of large deflection the von Karman's assumptions are employed. Therefore, the perturbed displacement gradients are also so small that the terms $\bar{\sigma}_{ij}\bar{u}_{s,j}$ may be dropped out except for $\bar{\sigma}_{ix}\bar{u}_{z,x}$ and $\bar{\sigma}_{iy}\bar{u}_{z,y}$. In order to give clarity to the integration procedure, Eq. (1) is written up as follows:

$$\partial(\sigma_{ij}\partial\bar{u}_x/\partial x_j)/\partial x_i + \partial\bar{\sigma}_{ix}/\partial x_i + \bar{F}_x + \Delta F_x = \rho\ddot{\bar{u}}_x, \tag{3}$$

$$\partial(\sigma_{ij}\partial\bar{u}_y/\partial x_j)/\partial x_i + \partial\bar{\sigma}_{iy}/\partial x_i + \bar{F}_y + \Delta F_y = \rho\ddot{\bar{u}}_y, \tag{4}$$

$$\partial(\sigma_{ij}\partial\bar{u}_z/\partial x_j)/\partial x_i + \partial\bar{\sigma}_{iz}/\partial x_i + \partial(\bar{\sigma}_{ix}\bar{u}_{z,x})/\partial x_i + \partial(\bar{\sigma}_{iy}\bar{u}_{z,y})/\partial x_i + \bar{F}_z + \Delta F_z = \rho\ddot{\bar{u}}_z. \tag{5}$$

3. Governing equations

The constitutive relations for each layer with respect to the laminate co-ordinate axes are given by

$$\begin{bmatrix} \bar{\sigma}_{xx} \\ \bar{\sigma}_{yy} \\ \bar{\sigma}_{zz} \\ \bar{\sigma}_{yz} \\ \bar{\sigma}_{zx} \\ \bar{\sigma}_{xy} \end{bmatrix} = \begin{bmatrix} C_{11} & C_{12} & C_{13} & 0 & 0 & C_{16} \\ C_{12} & C_{22} & C_{23} & 0 & 0 & C_{26} \\ C_{13} & C_{23} & C_{33} & 0 & 0 & C_{36} \\ 0 & 0 & 0 & C_{44} & C_{45} & 0 \\ 0 & 0 & 0 & C_{45} & C_{55} & 0 \\ C_{16} & C_{26} & C_{36} & 0 & 0 & C_{66} \end{bmatrix} \begin{bmatrix} \bar{\varepsilon}_{xx} \\ \bar{\varepsilon}_{yy} \\ \bar{\varepsilon}_{zz} \\ \bar{\varepsilon}_{yz} \\ \bar{\varepsilon}_{zx} \\ \bar{\varepsilon}_{xy} \end{bmatrix}. \tag{6}$$

The displacements of Reissner–Mindlin theory are assumed to be the following forms:

$$\bar{u}_x(x, y, z, t) = u_x(x, y, t) + z\varphi_x(x, y, t), \tag{7}$$

$$\bar{u}_y(x, y, z, t) = u_y(x, y, t) + z\varphi_y(x, y, t), \tag{8}$$

$$\bar{u}_z(x, y, z, t) = w(x, y, t). \tag{9}$$

The von Karman's assumptions are employed. In the strain and displacement relations, the retained non-linear terms are that which depend on $\bar{u}_{z,x}$ and $\bar{u}_{z,y}$. The other non-linear terms

are neglected

$$\begin{aligned}
\bar{\varepsilon}_{xx} &= \bar{u}_{x,x} + \tfrac{1}{2}\bar{u}_{z,x}^2,\\
\bar{\varepsilon}_{yy} &= \bar{u}_{y,y} + \tfrac{1}{2}\bar{u}_{z,y}^2,\\
\bar{\varepsilon}_{zz} &= \bar{u}_{z,z},\\
\bar{\varepsilon}_{yz} &= \bar{u}_{y,z} + \bar{u}_{z,y},\\
\bar{\varepsilon}_{zx} &= \bar{u}_{z,x} + \bar{u}_{x,z},\\
\bar{\varepsilon}_{xy} &= \bar{u}_{x,y} + \bar{u}_{y,x} + \bar{u}_{z,x}\bar{u}_{z,y}.
\end{aligned} \tag{10}$$

Substituting Eqs. (7)–(10) into the constitutive relations equations (6), the stress–displacement relations are as follows:

$$\begin{aligned}
\bar{\sigma}_{xx} = {} & C_{11}(u_{x,x} + z\varphi_{x,x} + w_{,x}^2/2) + C_{12}(u_{y,y} + z\varphi_{y,y} + w_{,y}^2/2)\\
& + C_{16}(u_{x,y} + z\varphi_{x,y} + u_{y,x} + z\varphi_{y,x} + w_{,x}w_{,y}),
\end{aligned} \tag{11}$$

$$\begin{aligned}
\bar{\sigma}_{yy} = {} & C_{12}(u_{x,x} + z\varphi_{x,x} + w_{,x}^2/2) + C_{22}(u_{y,y} + z\varphi_{y,y} + w_{,y}^2/2)\\
& + C_{26}(u_{x,y} + z\varphi_{x,y} + u_{y,x} + z\varphi_{y,x} + w_{,x}w_{,y}),
\end{aligned} \tag{12}$$

$$\begin{aligned}
\bar{\sigma}_{xy} = {} & C_{66}(u_{x,y} + z\varphi_{x,y} + u_{y,x} + z\varphi_{y,x} + w_{,x}w_{,y}) + C_{16}(u_{x,y} + z\varphi_{x,y} + w_{,x}^2/2)\\
& + C_{26}(u_{y,x} + z\varphi_{y,x} + w_{,y}^2/2),
\end{aligned} \tag{13}$$

$$\bar{\sigma}_{xz} = C_{44}(\varphi_x + w_{,x}) + C_{45}(\varphi_y + w_{,y}), \tag{14}$$

$$\bar{\sigma}_{yz} = C_{45}(\varphi_x + w_{,x}) + C_{55}(\varphi_y + w_{,y}). \tag{15}$$

Considering the equations of motion, the following initial stress resultants and material parameters of n-layer laminated plate are defined:

$$C_{ij} = \int_{-h/2}^{-(n-1)h/n} C_{ij} + \int_{-(n-1)h/n}^{-(n-2)h/n} C_{ij} + \cdots + \int_{(n-2)h/n}^{(n-1)h/n} C_{ij} + \int_{(n-1)h/n}^{h/2} C_{ij},$$

$$(A_{ij}, B_{ij}, D_{ij}) = \int C_{ij}(1, z, z^2)\,\mathrm{d}z \quad (i,\ j = 1,2,3,4,5,6),$$

$$(N_{ij}, M_{ij}) = \int \sigma_{ij}(1, z)\,\mathrm{d}z \quad (i,\ j = x, y, z),$$

$$I_1 = \int \rho\,\mathrm{d}z.$$

Here all the integral ranges are the whole thickness of the plate, i.e., from $-h/2$ to $h/2$. The N_{ij} and M_{ij} are stresses and moment resultants, respectively, and A_{ij}, B_{ij} and D_{ij} are the extension, extension–bending coupling and bending stiffness coefficients. The five governing equations can be obtained by substituting Eqs. (11)–(15) into Eqs. (3)–(5) and then integrating the equations.

These governing equations are as follows:

$$(L_1 + N_1 + R_1 + R_2)_{,x} + (L_5 + N_3 + S_1 + S_2)_{,y} + f_x = I_1 \ddot{u}_x, \tag{16}$$

$$(L_5 + N_3 + R_3)_{,x} + (L_2 + N_2 + S_3)_{,y} + f_y = I_1 \ddot{u}_y, \tag{17}$$

$$(L_6 + N_4 + N_5 + R_4)_{,x} + (L_7 + N_6 + N_7 + S_4)_{,y} + f_z = I_1 \ddot{w}, \tag{18}$$

$$(L_3 + N_8 + R_5 + R_6)_{,x} + (L_8 + N_{10} + S_5 + S_6)_{,y} - L_6 - R_8 + m_x = I_1 \ddot{\varphi}_x, \tag{19}$$

$$(L_8 + N_{10} + R_7)_{,x} + (L_4 + N_9 + S_7)_{,y} - L_7 - R_9 + m_y = I_1 \varphi_y. \tag{20}$$

The coefficients of above equations are given in Appendix A. The five boundary traction conditions for the x- and y-constant edges are derived by the same procedure as the governing equations and they will be shown in the example problem.

4. Example problem

Here a simply supported laminated hybrid composite plate of uniform thickness h in a state of initial stress is to be considered, as shown in Fig. 1. The state of initial stresses is

$$\sigma_{xx} = \sigma_n + 2z\sigma_m/h, \tag{21}$$

where σ_m and σ_n are taken to be constant and other initial stresses assumed to be zero. It is, therefore, a composite of tensile (compressive) σ_n and bending stress σ_m.

Lateral loads and body forces are taken to be zero:

$$f_x, f_y, f_z, m_x, m_y = 0.$$

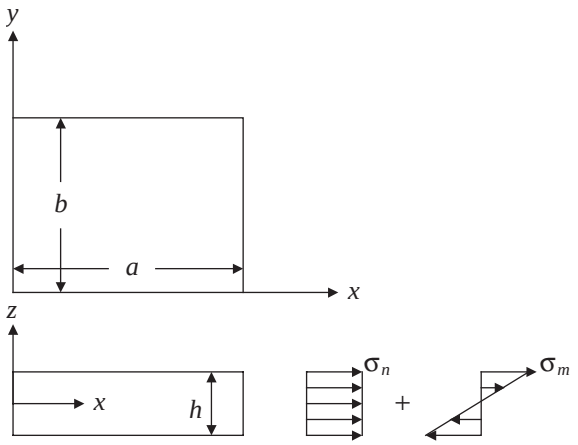

Fig. 1. A simply supported laminated hybrid composite plate with initial stress.

The boundary conditions are, on the $x = 0$ and a edges,

$$u_y = 0, \quad w = 0,$$
$$\bar{F}_{xx} + \Delta F_{xx} = L_1 + N_1 + R_1 + R_2,$$
$$\bar{M}_{xx} + \Delta M_{xx} = L_3 + N_8 + R_5 + R_6 \tag{22}$$

on the $y = 0$ and b edges,

$$u_x = 0, \quad w = 0$$
$$\bar{F}_{yy} + \Delta F_{yy} = L_2 + N_2 + S_3,$$
$$\bar{M}_{yy} + \Delta M_{yy} = L_4 + N_9 + S_7, \tag{23}$$

where

$$(\bar{F}_{ii}, \bar{M}_{ii}) = \int \bar{P}_i(1, z)\,\mathrm{d}z$$
$$(\Delta F_{ii}, \Delta M_{ii}) = \int \Delta P_i(1, z)\,\mathrm{d}z.$$

$\bar{P}_i$ is the applied surface tractions, $\Delta\bar{P}_i$ represents the changes of initial surface traction. The following one-term fundamental mode shapes satisfy the boundary conditions Eqs. (22) and (23)

$$u_x = hU(t)\cos(\pi x/a)\sin(\pi y/b),$$
$$u_y = hV(t)\sin(\pi x/a)\cos(\pi y/b),$$
$$w = hW(t)\sin(\pi x/a)\sin(\pi y/b),$$
$$\varphi_x = \Psi_x(t)\cos(\pi x/a)\sin(\pi y/b),$$
$$\varphi_y = \Psi_y(t)\sin(\pi x/a)\cos(\pi y/b). \tag{24}$$

Substituting the assumed displacement fields of Eq. (24) into the equations of motion (16)–(20) and solving the equations by Galerkin method, one obtains

$$C_{1,1}U + C_{1,2}V + C_{1,4}\Psi_x + N_1^* W^2 = \ddot{U}, \tag{25}$$

$$C_{1,2}U + C_{2,2}V + C_{2,5}\Psi_y + N_2^* W^2 = \ddot{V}, \tag{26}$$

$$C_{3,3}W + C_{3,4}\Psi_x + C_{3,5}\Psi_y + N_3^* UW + N_4^* VW + N_5^* W^3 = \ddot{W}, \tag{27}$$

$$C_{1,4}U + C_{3,4}W + C_{4,4}\Psi_x + C_{4,5}\Psi_y + N_6^* W^2 = \ddot{\Psi}_x/12, \tag{28}$$

$$C_{2,5}V + C_{3,5}W + C_{4,5}\Psi_x + C_{5,5}\Psi_y + N_7^* W^2 = \ddot{\Psi}_y/12. \tag{29}$$

The coefficients of above equations are given in Appendix B, and the shear correction factor was introduced into $C_{4,4}$ and $C_{5,5}$ [28].

The equations are integrated by using the fourth order Runge–Kutta method with the non-dimensional time step of 0.001. In each case, the initial conditions are chosen as

$$U(0) = V(0) = \Psi_x(0) = \Psi_y(0) = 0, \quad W(0) = W_{max},$$

$$U_{,t}(0) = V_{,t}(0) = \Psi_{x,t}(0) = \Psi_{y,t}(0) = W_{,t}(0) = 0.$$

The initial in-plane compressive (tensile) stress is included in the buckling coefficient K. If K is positive, then the stress is tensile. The initial in-plane bending stress is included in β, when $\beta = 0$ there is no initial bending stress. The non-linear frequency for one full cycle is measured as ω_{nl}. The linear frequency ω_l can be calculated by neglecting the non-linear terms in Eqs. (25)–(29).

5. Result and discussion

This study investigates the behavior of flexural mode in plate vibration. The non-linear vibration behavior is described as the vibration frequency ratio of non-linear to linear, i.e., ω_{nl}/ω_l. The frequency ratio is affected by the vibration amplitude, material property and initial stress. To verify the accuracy of present computer program, the frequency ratios with no initial stress are studied first. The comparison for an isotropic plate with no initial stress was performed for verification. The calculated frequency ratios at various values of W_{max} were listed in Table 1. Agreement can be seen when present results are compared to the results of Singh et al. [29] and Sathymoorthy [4]. However, present results are little larger than Sathymoorthy's and Singh's findings on high vibration amplitudes, and the difference in increases with respect to the increase in vibration amplitude. It is owing to the neglect of some terms in Sathymoorthy's and Singh's governing equations. If present method ignores the $(\bar{\sigma}_{xx})_{,x}w_{,x}$, $(\bar{\sigma}_{yy})_{,y}w_{,y}$, $(\bar{\sigma}_{xy})_{,y}w_{,x}$, $(\bar{\sigma}_{xy})_{,x}w_{,y}$ and in-plane inertia terms, then it will be the same as Sathymoorthy's. On the other hand, the difference between present method and Singh's is the higher order terms. The present formulas were applied to glass epoxy and graphite epoxy plates with orthotropic properties. Table 2 shows

Table 1
Comparison of frequency ratios of isotropic square plate ($a/b = 1$, $a/h = 10$, $K = 0$, $\beta = 0$)

W_{max}	Vibration frequency ratios		
	Singh's results [29]	Sathymoorthy's results [4]	Present results
0.2	1.023	1.028	1.033
0.4	1.090	1.104	1.129
0.6	1.192	1.220	1.280
0.8	1.321	1.364	1.453
1.0	1.468	1.527	1.658

Table 2
Comparison of frequency ratios of orthotropic square plate ($a/b = 1$, $a/h = 10$, $K = 0$, $\beta = 0$)

W_{max}	Glass fiber polymer		Carbon fiber polymer	
	Singh's results [8]	Present results	Singh's results [8]	Present results
0.3	1.0668	1.0692	1.0836	1.0885
0.6	1.2460	1.2517	1.3027	1.3159
0.9	1.4978	1.5049	1.6026	1.6224
1.2	1.7918	1.8134	1.9463	1.9714
1.5	2.1104	2.1415	2.3143	2.3470

Table 3
Comparison of frequency ratios of two layered cross-ply plate ($a/b = 1$, $a/h = 80$, $E_1/E_2 = 40$, $G_{12}/E_2 = 0.5$, $\upsilon_{12} = 0.25$, $K = 0$, $\beta = 0$)

W_{max}	Vibration frequency ratios		
	Singh's results [9]	Results of the classical plate equations	Present results
0.3	1.0796	1.0762	1.0812
0.6	1.2867	1.2752	1.3019
0.9	1.5691	1.5534	1.6094
1.2	1.8933	1.8778	1.9418
1.5	2.2414	2.2299	2.2919
1.8	2.6040	2.6001	2.6715
2.1	2.9759	2.9787	3.1024

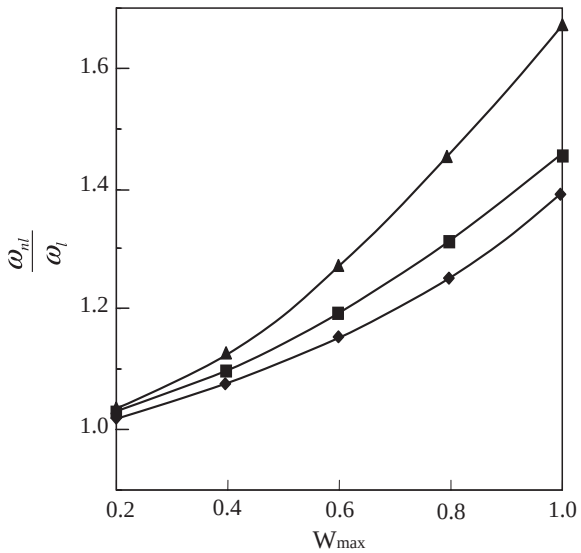

Fig. 2. Comparison of frequency ratios of hybrid composite plate. (◆: Lee's result [16]; ▩: results of the classical plate equations; ▲: present results.)

the results and it can be observed that the data are quite in agreement with Singh's results [8]. The frequency ratios of two-layer cross-ply and four-layer hybrid composite plates for various vibration amplitudes are given in Table 3 and Fig. 2, respectively. Besides, Singh's results [9], Lee's results [16] and the results of the classical plate equations obtained by simplifying the current plate governing equations are also presented for comparison. It can be observed that the results agree well with each other at all vibration amplitudes, and the vibration frequency ratio increases with the vibration amplitude. However, present study includes the effects of transverse shear and rotary inertia that are not considered in the classical theory. This makes the vibration frequency ratio larger than the result of classical theory. The difference between present results and classical plate theory results increases with the increasing of vibration amplitude. The accuracy of the

Table 4
Comparison of linear frequency of initial stressed isotropic plate ($a/b = 1$, $\upsilon_{12} = 0.3$, $K = -2$, $\beta = 0$)

a/h	Linear frequency	
	Doong's results [30]	Present results
10	0.0634	0.0634
20	0.0167	0.0167
30	0.0075	0.0075
40	0.0043	0.0043
50	0.0027	0.0027

Table 5
Material properties of ingredients of laminated hybrid composite plates

	E_1 (GPa)	E_2 (GPa)	G_{12} (GPa)	υ_{12}
Aluminum (Al)	72.0	72.0	28.0	0.33
CFRP	181.0	10.3	7.17	0.28
GFRP	38.6	8.27	4.14	0.26

Table 6
The ingredients and laminate stacking sequences of different laminated hybrid composite plates

	Laminate stacking sequence	Symmetry
Plate A	Al/CFRP(0°)/CFRP(90°)/Al	No
Plate B	Al/CFRP(0°)/CFRP(0°)/Al	Yes
Plate C	Al/GFRP(0°)/GFRP(90°)/Al	No
Plate D	Al/GFRP(0°)/GFRP(0°)/Al	Yes
Plate E	CFRP(0°)/Al/Al/CFRP(90°)	No
Plate F	CFRP(0°)/Al/Al/CFRP(0°)	Yes

proposed method for initially stressed plates can be ensured from the comparison in Table 4. The linear frequencies of present method agree with those previously published [30] for an isotropic plate sustaining a compressive stress ($K = -2$).

Table 5 lists the material properties of the ingredients of laminated hybrid composite plates investigated in this study. The ingredients and laminate stacking sequences of different laminated hybrid composite plates are listed in Table 6. The vibration frequency ratios of various plates at different vibration amplitudes are presented in Table 7. The effects of different ingredients on the vibration frequency ratio can be observed. The vibration frequency ratios of aluminum carbon fiber reinforced polymer (CFRP) hybrid composite plates (plates A and B) are larger than those of aluminum glass fiber reinforced polymer (GFRP) hybrid composite plates (plates C and D). This could be attributed to that the elastic modulus of CFRP is higher than that of GFRP. The effects of laminate stacking sequences on the vibration frequency ratio can also be observed. The

Table 7
Comparison of frequency ratios of various plates at different vibration amplitudes ($a/b = 1$, $a/h = 10$, $K = 0$, $\beta = 0$)

W_{max}	Vibration frequency ratios					
	Plate A	Plate B	Plate C	Plate D	Plate E	Plate F
0.2	1.0105	1.0687	1.0100	1.0262	1.0486	1.1268
0.4	1.1052	1.1632	1.0790	1.0909	1.1410	1.3138
0.6	1.2285	1.2929	1.1738	1.1867	1.3812	1.5904
0.8	1.3824	1.4548	1.3007	1.3150	1.6924	1.9481
1.0	1.5778	1.6605	1.4479	1.4638	2.0238	2.3302

Table 8
Comparison of vibration frequency ratios of various hybrid composite plates with an initial compressive stress at different vibration amplitudes ($a/b = 1$, $a/h = 10$, $K = -2$, $\beta = 0$)

W_{max}	Vibration frequency ratios			
	Plate A	Plate B	Plate C	Plate D
0.2	1.0462	1.1038	1.0384	1.0691
0.4	1.2624	1.3105	1.1533	1.1874
0.6	1.3231	1.6425	1.3343	1.3737
0.8	1.5945	1.9826	1.5616	1.6076
1.0	1.9094	2.3741	1.8173	1.8309

vibration frequency ratios of symmetric hybrid composite plates (plates B, D and F) are larger than those of unsymmetric hybrid composite plates (plates A, C and E). However, for aluminum/CFRP hybrid composite plates, the difference of vibration frequency ratios between unsymmetric and symmetric hybrid composite plates (plates A and B; plates E and F) is significant. The difference is quite small between unsymmetric and symmetric aluminum/GFRP hybrid composite plates (plates C and D). On the other hand, the frequency ratios of plates E and F that aluminum is stacked in the inner layers of laminated hybrid composite plate are larger than those of plates A and B that aluminum is stacked at the outer surfaces.

Table 8 lists the vibration frequency ratios of various plates with an initial compressive stress at different vibration amplitudes. It can be seen that the frequency ratios of plates with an initial compressive stress are larger than those in Table 7 where plates are not subjected to an initial stress. Besides, the frequency ratios of plate B are still larger than those of plates A, C and D because plate B is composed of aluminum and high elastic modulus CFRP as well as symmetrically stacked. The effects of initial stresses on the frequency ratios with various vibration amplitudes are further examined in Fig. 3. It is observed that as compared with the plate with no initial stress, an initial compressive stressed plate ($K < 0$) has larger frequency ratios while an initial tensile stressed plate ($K > 0$) has smaller results.

Fig. 4 depicts the effect of initial stress on the vibration frequency ratio for different plates. The buckling coefficient is obtained when the inverse of frequency ratio approaches zero, i.e., $\omega_l/\omega_{nl} = 0$. It can be seen that the plates A and B has smaller absolute values of buckling

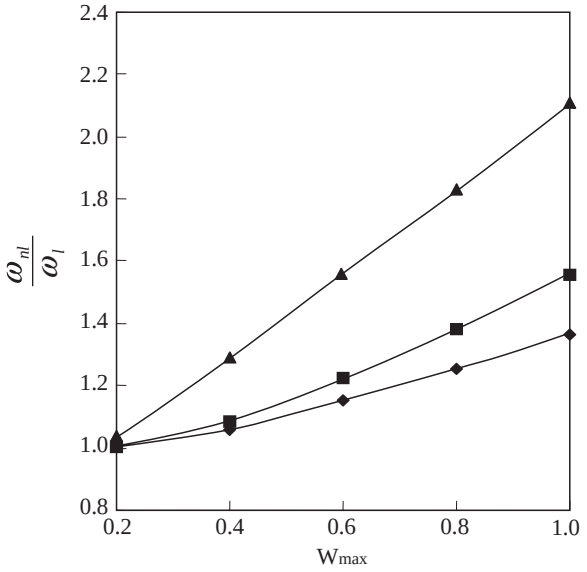

Fig. 3. The effects of initial stresses (♦: $K = 2$; ▩ $K = 0$; ▲: $K = -2$) on the frequency ratios of plate A ($a/b = 1$, $a/h = 10$, $\beta = 0$) at various vibration amplitudes.

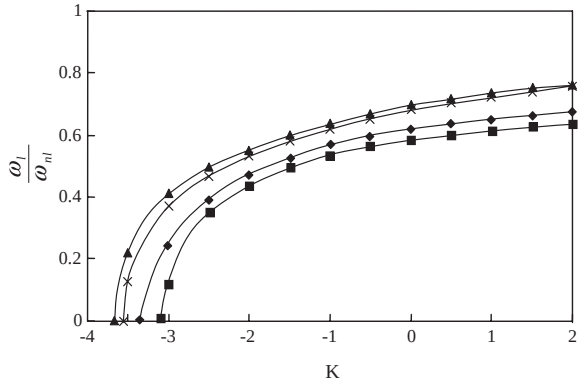

Fig. 4. The effect of initial stress on the vibration frequency ratio for different plates of $a/b = 1$, $a/h = 10$, $\beta = 0$. (♦: plate A; ▩: plate B; ▲: plate C; ×: plate D.)

coefficient than plates C and D have, although the elastic modulus of plates A and B is higher than those of plates C and D.

Table 9 presents the effect of initial bending stress on the vibration frequency ratio. It can be seen that bending stress increases the vibration frequency ratio, as compared with Table 8; however, the effect is not very obvious at low bending stresses. Besides, as the initial bending stress is included in the ratio of bending stress to uniform normal stress, i.e., β the larger the ratio is, the larger the vibration frequency ratio is. However, if the effects of initial bending stresses on

Table 9
The effect of initial bending stress on the vibration frequency ratio ($a/b = 1$, $a/h = 10$, $K = -2$, $w_{\max} = 1$)

β	Vibration frequency ratios			
	Plate A	Plate B	Plate C	Plate D
0	1.9094	2.3741	1.8173	1.8309
10	1.9515	2.3721	1.8260	1.8691
20	2.1562	2.3809	1.8452	1.8741
30	2.2116	2.3990	1.8779	1.8971
40	2.3230	2.4266	1.9226	1.9372
50	2.4167	2.4743	1.9816	1.9715

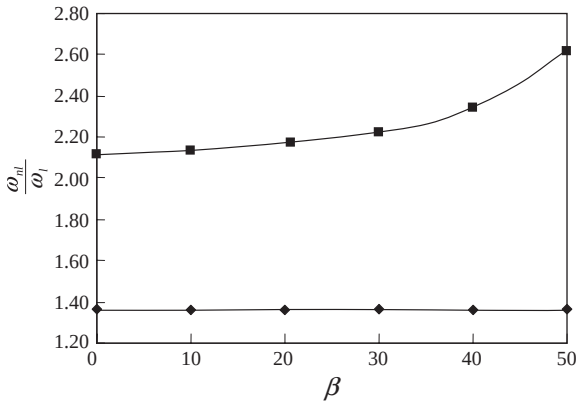

Fig. 5. The effects of initial bending stresses (◆: $K = 2$; ▩: $K = -2$) on the vibration frequency ratio of plate A ($a/b = 1$, $a/h = 10$, $W_{max} = 1$) under different in-plane uniform normal stresses.

the vibration frequency ratio are further examined under different in-plane uniform normal stresses, as shown in Fig. 5, it can be seen that the increase of bending stress has much less influence on the frequency ratio under initial tensile stress.

6. Conclusion

Non-linear vibrating behaviors of initially stressed laminated hybrid composite plates have been described and discussed. The preliminary results are summarized as follows:

(1) The plate vibration frequency ratios obtained from present study are larger than those from the classical theory. It is due to the effects of transverse shear and rotary inertia that are not considered in the classical theory.
(2) The vibration frequency ratio increases with the vibration amplitude and elastic modulus. The vibration frequency ratios of aluminum/CFRP hybrid composite plates are larger than those

of aluminum/GFRP hybrid composite plates as the elastic modulus of CFRP is higher than that of GFRP.

(3) The laminate stacking sequence influences the vibration frequency ratio. The vibration frequency ratios of symmetric hybrid composite plates are larger than those of unsymmetric plates. The laminated plates that aluminum is stacked in the inner layers have larger frequency ratios than those plates that aluminum is stacked at the outer surfaces.

(4) The plates laminated with higher elastic modulus material have smaller absolute values of buckling coefficient.

(5) The larger the ratio of bending stress to uniform normal stress is, the larger the vibration frequency ratio is under initial uniform compressive stress, but the bending stress almost does not affect the frequency ratio under initial uniform tensile stress.

Appendix A

$$
\begin{aligned}
L_1 &= A_{11}u_{x,x} + A_{12}u_{y,y} + A_{16}(u_{x,y} + u_{y,x}) + B_{11}\varphi_{x,x} + B_{12}\varphi_{y,y} + B_{16}(\varphi_{x,y} + \varphi_{y,x}),\\
L_2 &= A_{12}u_{x,x} + A_{22}u_{y,y} + A_{26}(u_{x,y} + u_{y,x}) + B_{12}\varphi_{x,x} + B_{22}\varphi_{y,y} + B_{26}(\varphi_{x,y} + \varphi_{y,x}),\\
L_3 &= B_{11}u_{x,x} + B_{12}u_{y,y} + B_{16}(u_{x,y} + u_{y,x}) + D_{11}\varphi_{x,x} + D_{12}\varphi_{y,y} + D_{16}(\varphi_{x,y} + \varphi_{y,x}),\\
L_4 &= B_{12}u_{x,x} + B_{22}u_{y,y} + B_{26}(u_{x,y} + u_{y,x}) + D_{12}\varphi_{x,x} + D_{22}\varphi_{y,y} + D_{26}(\varphi_{x,y} + \varphi_{y,x}),\\
L_5 &= A_{16}u_{x,x} + A_{26}u_{y,y} + A_{66}(u_{x,y} + u_{y,x}) + B_{16}\varphi_{x,x} + B_{26}\varphi_{y,y} + B_{66}(\varphi_{x,y} + \varphi_{y,x}),\\
L_6 &= A_{45}(w_{,y} + \varphi_y) + A_{55}(w_{,x} + \varphi_x),\\
L_7 &= A_{44}(w_{,y} + \varphi_y) + A_{45}(w_{,x} + \varphi_x),\\
L_8 &= B_{16}u_{x,x} + B_{26}u_{y,y} + B_{66}(u_{x,y} + u_{y,x}) + D_{16}\varphi_{x,x} + D_{26}\varphi_{y,y} + D_{66}(\varphi_{x,y} + \varphi_{y,x}),
\end{aligned}
$$

$$
\begin{aligned}
N_1 &= A_{11}w_{,x}^2/2 + A_{12}w_{,y}^2/2 + A_{16}w_{,x}w_{,y},\\
N_2 &= A_{12}w_{,x}^2/2 + A_{22}w_{,y}^2/2 + A_{26}w_{,x}w_{,y},\\
N_3 &= A_{16}w_{,x}^2/2 + A_{26}w_{,y}^2/2 + A_{66}w_{,x}w_{,y},\\
N_4 &= (L_1 + N_1)w_{,x},\\
N_5 &= (L_5 + N_3)w_{,x},\\
N_6 &= (L_2 + N_2)w_{,y},\\
N_7 &= (L_5 + N_3)w_{,y},\\
N_8 &= B_{11}w_{,x}^2/2 + B_{12}w_{,y}^2/2 + B_{16}w_{,x}w_{,y},\\
N_9 &= B_{12}w_{,x}^2/2 + B_{22}w_{,y}^2/2 + B_{26}w_{,x}w_{,y},\\
N_{10} &= B_{16}w_{,x}^2/2 + B_{26}w_{,y}^2/2 + B_{66}w_{,x}w_{,y},
\end{aligned}
$$

$$
\begin{aligned}
R_1 &= N_{xx}u_{x,x} + M_{xx}\varphi_{x,x},\\
R_2 &= N_{xy}u_{x,y} + M_{xy}\varphi_{x,y} + N_{xz}u_{z,x},
\end{aligned}
$$

$$
\begin{aligned}
R_3 &= N_{xx}u_{y,x} + M_{xx}\varphi_{y,x} + N_{xy}u_{y,y} + M_{xy}\varphi_{y,y} + N_{xz}u_{z,y},\\
R_4 &= N_{xx}w_{,x} + N_{xy}w_{,y},\\
R_5 &= M_{xx}u_{x,x},\\
R_6 &= M_{xy}u_{x,y} + M_{xz}u_{z,x},\\
R_7 &= M_{xx}u_{y,x} + M_{xy}u_{y,y} + M_{xz}u_{z,y},\\
R_8 &= N_{xz}u_{x,x} + M_{xz}\varphi_{x,x} + N_{zz}\varphi_x + N_{zy}u_{x,y} + M_{zy}\varphi_{x,y},\\
R_9 &= N_{xz}u_{y,x} + M_{xz}\varphi_{y,x} + N_{zz}\varphi_{yx} + N_{zy}u_{y,y} + M_{zy}\varphi_{y,y},
\end{aligned}
$$

$$
\begin{aligned}
S_1 &= N_{yy}u_{x,y} + M_{yy}\varphi_{x,y},\\
S_2 &= N_{xy}u_{x,x} + M_{xy}\varphi_{x,x} + N_{yz}u_{z,x},\\
S_3 &= N_{yy}u_{y,y} + M_{yy}\varphi_{y,y} + N_{xy}u_{y,x} + M_{xy}\varphi_{y,x} + N_{xz}u_{z,y},\\
S_4 &= N_{xy}w_{,x} + N_{yy}w_{,y},\\
S_5 &= M_{yy}u_{x,y},\\
S_6 &= M_{xy}u_{x,x} + M_{yz}u_{z,x},\\
S_7 &= M_{yy}u_{y,y} + M_{xy}u_{y,x} + M_{xz}u_{z,y},
\end{aligned}
$$

$$
\begin{aligned}
f_x &= \int_{-h/2}^{h/2} (\bar{X}_x + \Delta X_x)\,\mathrm{d}z + \sigma_{zx}^{+} - \sigma_{zx}^{-},\\
f_y &= \int_{-h/2}^{h/2} (\bar{X}_y + \Delta X_y)\,\mathrm{d}z + \sigma_{zy}^{+} - \sigma_{zy}^{-},\\
f_z &= \int_{-h/2}^{h/2} (\bar{X}_z + \Delta X_z)\,\mathrm{d}z + (\sigma_{zx}^{+} - \sigma_{zx}^{-})w_{,x} + (\sigma_{zy}^{+} - \sigma_{zy}^{-})w_{,y} + \sigma_{zz}^{+} - \sigma_{zz}^{-},
\end{aligned}
$$

$$
\begin{aligned}
m_x &= \int_{-h/2}^{h/2} (\bar{X}_x + \Delta X_x)z\,\mathrm{d}z + h(\sigma_{zx}^{+} - \sigma_{zx}^{-})/2,\\
m_y &= \int_{-h/2}^{h/2} (\bar{X}_y + \Delta X_y)z\,\mathrm{d}z + h(\sigma_{zy}^{+} - \sigma_{zy}^{-})/2.
\end{aligned}
$$

Appendix B

$$
\begin{aligned}
C_{1,1} &= -(12 + A_{66}h^2R^2/D_{11} + FK),\\
C_{1,2} &= -(A_{12}h^2 + A_{66}h^2)R/D_{11},\\
C_{1,4} &= -(B_{11} + B_{66}R^2)h/D_{11} + \beta FK/6,\\
C_{1,5} &= -(B_{12} + B_{66})hR/D_{11},\\
C_{2,2} &= -(A_{66} + A_{22}R^2)h^2/D_{11},
\end{aligned}
$$

$$C_{2,4} = C_{1,5}, \quad C_{2,5} = C_{1,4},$$
$$C_{3,3} = -(A_{55}h^2/D_{11} + A_{44}h^2R^2/D_{11} + FK),$$
$$C_{3,4} = -A_{55}h^2r/(\pi D_{11}), \quad C_{3,5} = -A_{44}h^2Rr/(\pi D_{11}),$$
$$C_{4,4} = -(1 + D_{66}R^2/D_{11} + A_{55}h^2r^2/(\pi^2 D_{11}) + FK/12),$$
$$C_{4,5} = A_{13}h^2r/(\pi D_{11}) - (D_{12} + D_{66})R/D_{11},$$
$$C_{5,5} = -(D_{66}/D_{11} + D_{22}R^2/D_{11} + A_{44}h^2r^2/(\pi^2 D_{11}) + FK/12),$$

$$F = \pi^2R^2/r^2, \quad K = N_{xx}b^2/hD_{11}, \quad \tau = t(\pi^2 D_{11}/\rho h^3 a^2)^{1/2},$$

$$R = a/b, \quad r = a/h, \quad \beta = \sigma_m/\sigma_n,$$

$$N_1^* = 16/(9\pi^2 rD_{11})(-2A_{11}h^2 + A_{12}h^2R^2 - A_{66}h^2R^2),$$
$$N_2^* = 16/(9\pi rD_{11})(-A_{66}h^2R + A_{12}h^2R - 2A_{22}h^2R^3),$$
$$N_3^* = -N_1^*/\pi, \quad N_4^* = 2N_2^*,$$
$$N_5^* = -\pi^2/(32r^2D_{11})(9A_{11}h^2 + 2A_{12}h^2R^2 + 4A_{66}h^2R^4 + 9A_{22}h^2R^4),$$
$$N_6^* = 16/(9\pi^2 rD_{11})(-2B_{11}h^2 + B_{12}h^2R^2 - B_{66}h^2R^2),$$
$$N_7^* = 16/(9\pi rD_{11})(-B_{66}h^2R + B_{12}h^2R - 2B_{22}h^2R^3).$$

Appendix C. Nomenclature

A_{ij}, B_{ij}, D_{ij}	stiffness of plate
C_{ij}	stiffness coefficients of stress–strain relations
$\bar{u}_i$	displacements of plate in x, y, z directions
u_x, u_y, w	displacements of plate ($z = 0$) in x, y, z directions
φ_x, φ_y	rotations of plate in x, y directions
I_1	the inertia coefficients of plate
a, b	dimensions of plate in x, y directions
h	plate thickness
R	aspect ratio, $R = a/b$
r	thickness ratio, $r = a/h$
W_{max}	non-dimensional vibration amplitude, $W_{max} = w/h$
N_{ij}, M_{ij}	initial stress resultants
$\bar{P}_i, \Delta P_i$	the applied surface traction and perturbing surface traction
σ_m	in-plane bending stress
σ_n	in-plane uniform normal stress
β	ratio of bending stress to uniform normal stress, $\beta = \sigma_m/\sigma_n$
K	non-dimensional buckling coefficient, $K = N_{xx}b^2/hD_{11}$
τ	non-dimensional time, $\tau = t(\pi^2 D_{11}/\rho h^3 a^2)$
ω_l	non-dimensional linear frequency

ω_{nl} non-dimensional non-linear frequency
E_1, E_2 Young's modulus in layer material directions
G_{12}, G_{23} shear modulus with respect to layer material directions

References

[1] R. Chandra, Large deflection vibration of cross-ply laminated plates with certain edge condition, *Journal of Sound and Vibration* 47 (1976) 509–514.
[2] R. Chandra, B.B. Raju, Large deflection vibration of angle ply laminated plates, *Journal of Sound and Vibration* 40 (1975) 393–408.
[3] H.K. Berger, New approach to the analysis of large deflections of plates, *Journal of Applied Mechanics* 22 (1955) 465–472.
[4] M. Sathymoorthy, Effects of large amplitude shear and rotary inertia on vibration of rectangular plates, *Journal of Sound and Vibration* 63 (1979) 161–167.
[5] J.N. Reddy, W.C. Chao, Non-linear oscillations of laminated, anisotropic, rectangular plates, *Transactions of the American Society of Mechanical Engineers* 49 (1982) 396–402.
[6] J.N. Reddy, C.L. Huang, L.R. Singh, Large deflections and large amplitude vibrations of axisymmetric circular plates, *International Journal for Numerical Methods in Engineering* 17 (1981) 527–541.
[7] K.S. Sivakumaran, C.Y. Chia, Large-amplitude oscillations of unsymmetrically laminated anisotropic rectangular plates including shear, rotatory inertia, and transverse normal stress, *Transactions of the American Society of Mechanical Engineers* 52 (1985) 536–542.
[8] G. Singh, K.K. Raju, G.V. Rao, Non-linear vibrations of simply supported rectangular cross-ply plates, *Journal of Sound and Vibration* 142 (1990) 213–226.
[9] G. Singh, G.V. Rao, Large amplitude free vibration of simply supported antisymmetric cross-ply plates, *American Institute of Aeronautics and Astronautics Journal* 29 (1991) 784–790.
[10] B.N. Rao, S.R.R. Pillai, Large-amplitude free vibrations of laminated anisotropic thin plates based on harmonic balance method, *Journal of Sound and Vibration* 154 (1992) 173–177.
[11] B.N. Rao, Large-amplitude free vibrations of simply supported uniform beams with immovable ends, *Journal of Sound and Vibration* 155 (1992) 523–527.
[12] J. Argyris, L. Tenek, L. Olofsson, Non-linear free vibrations of composite plates, *Computer Methods in Applied Mechanics and Engineering* 115 (1994) 1–15.
[13] A.V. Sinfh, Linear and Geometrically non-linear vibrations of fiber reinforced laminated plates and shallow shells, *Computer and Structures* 76 (2000) 277–285.
[14] J. Mackerle, Geometric-non-linear analysis by finite element and boundary element methods—a bibliography (1997–1998), *Finite Elements in Analysis and Design* 32 (1999) 51–62.
[15] J. Mackerle, Finite element linear and non-linear, static and dynamic analysis of structural elements—a bibliography (1992–1995), *Engineering Computation* 14 (1997) 347–440.
[16] Y.S. Lee, Y.W. Kim, Analysis of non-linear vibration of hybrid composite plates, *Computers and Structures* 61 (1996) 573–578.
[17] E.J. Brunell, S.R. Robertson, Initially stressed mindlin plates, *American Institute of Aeronautics and Astronautics Journal* 12 (1974) 1036–1045.
[18] E.J. Brunell, S.R. Robertson, Vibrations of an initially stressed thick plate, *Journal of Sound and Vibration* 45 (1976) 405–416.
[19] L.W. Chen, J.L. Doong, Large amplitude vibration of an initially stressed moderately thick plate, *Journal of Sound and Vibration* 89 (1983) 499–508.
[20] L.W. Chen, J.L. Doong, Large amplitude vibration of an initially stressed thick circular plate, *American Institute of Aeronautics and Astronautics Journal* 21 (1983) 1317–1324.
[21] C.S. Chen, J.Y. Lai, J.L. Doong, Large amplitude vibration of plates according to higher order deformation theory, *Journal of Sound and Vibration* 188 (1995) 149–166.

[22] C.S. Chen, J.R. Hwang, J.L. Doong, Non-linear vibration of an initially stressed plate based on a modified plate theory, *International Journal of Solids and Structures* 38 (2001) 8563–8583.
[23] J. Grawford, S. Atluri, Non-linear vibrations of a flat plate with initial stresses, *Journal of Sound and Vibration* 43 (1975) 117–129.
[24] Y.K. Cheung, D.S. Zhu, V.P. Iu, Non-linear vibration of thin plates with initial stress by spline finite strip method, *Thin-Walled Structures* 32 (1998) 275–287.
[25] N. Yamaki, M. Chiba, Non-linear vibrations of a clamped rectangular plate with initial deflection and initial edge displacement—part I: theory, *Thin-Walled Structures* 1 (1983) 3–29.
[26] N. Yamaki, K. Otomo, M. Chiba, Non-linear vibrations of a clamped rectangular plate with initial deflection and initial edge displacement—part II: experiment, *Thin-Walled Structures* 1 (1983) 101–119.
[27] V.V. Bolotin, *Non Conservative Problems of the Theory of Elastic Stability*, Macmillan, New York, 1963.
[28] C.W. Bert, F. Gordaninejad, Transverse shear effects in bimodular composite laminates, *Journal of Composite Materials* 17 (1983) 282–298.
[29] P.N. Singh, V. Sundarajan, Y.C. Das, Large amplitude vibration of same moderately thick structural elements, *Journal of Sound and Vibration* 36 (1974) 375–387.
[30] J.L. Doong, Vibration and stability of initially stressed thick plate according to a higher-order deformation theory, *Journal of Sound and Vibration* 113 (1987) 425–440.